Design, Synthesis, Evaluation and Structure of Allenic 1α,25-Dihydroxyvitamin D_3 Analogs with Locked Mobility at C-17

Ramón Fraga,[a] Kateryna Len,[b] Regis Lutzing,[b] Gilles Laverny,[b] Julian Loureiro,[c] Miguel A. Maestro,[a, d] Natacha Rochel,*[b] Enrique Rodriguez-Borges,*[c] and Antonio Mouriño*[a]

In memory of Anthony Norman and Gary Posner.

Abstract: Vitamin D receptor ligands have potential for the treatment of hyperproliferative diseases and disorders related to the immune system. However, hypercalcemic effects limit their therapeutical uses and call for the development of tissue-selective new analogs. We have designed and synthesized the first examples of 1α,25-dihydroxyvitamin D_3 analogs bearing an allenic unit attached to the D ring to restrict the side-chain conformational mobility. The triene system was constructed by a Pd^0-mediated cyclization/Suzuki-Miyaura cross-coupling process in the presence of an allenic side chain. The allenic moiety was built through an orthoester-Claisen rearrangement of a propargylic alcohol. The biological activity and structure of (22*S*)-1α,25-dihydroxy-17,20-dien-24-homo-21-nor-vitamin D_3 bound to binding domain of the vitamin D receptor, provide information concerning side-chain conformational requirements for biological activity.

Introduction

The active form of the secosteroid hormone vitamin D_3, 1α,25-dihydroxyvitamin D_3 [**1**, calcitriol, 1,25-$(OH)_2D_3$, 1,25D, Figure 1], exerts its biological functions by binding to the vitamin D receptor (VDR), a transcription factor of the nuclear receptor superfamily (NRs).[1] 1,25D was known for many years as a primary regulator of calcium homeostasis, but it also controls a wide range of other biological functions including cell differentiation, cell proliferation, and immune responses.[2,3] 1,25D induces the expression of more than 200 genes associated with several diseases such as arthritis, diabetes and cancer, suggesting that this secosteroid hormone might induce a wide range of biological functions.[4] Unfortunately, 1,25D induces hypercalce-

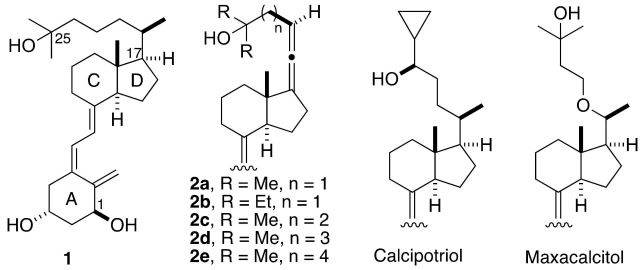

Figure 1. Structures of the natural hormone 1,25D (**1**), 1,25D analogs **2a**–**2e**, calcipotriol and maxacalcitol.

[a] *Dr. R. Fraga, Prof. M. A. Maestro, Prof. A. Mouriño*
Departamento de Química Orgánica
Laboratorio de Investigación Ignacio Ribas
Universidad de Santiago, Avda Ciencias s/n
15782 Santiago de Compostela (Spain)
E-mail: antonio.mourino@usc.es

[b] *K. Len, R. Lutzing, Dr. G. Laverny, Prof. N. Rochel*
Institut de Génétique et de Biologie, Moléculaire et Cellulaire (IGBMC)
67400 Illkirch (France)
and
Institut National de La Santé et de La Recherche Médicale (INSERM), U1258
67400 Illkirch (France)
and
Centre National de Recherche Scientifique (CNRS), UMR7104
67400 Illkirch (France)
and
Université de Strasbourg, 67400 Illkirch (France)
E-mail: rochel@igbmc.fr

[c] *Dr. J. Loureiro, Prof. E. Rodriguez-Borges*
LAQV/REQUIMTE
Departamento de Química e Bioquímica
Faculdade de Ciências da Universidade do Porto (Portugal)
E-mail: jrborges@fc.up.pt

[d] *Prof. M. A. Maestro*
Departamento de Química-CICA
Facultad de Ciencias
Universidad de A Coruña
Campus da Zapateira s/n, 15071 A Coruña (Spain)

Supporting information for this article is available on the WWW under https://doi.org/10.1002/chem.202101578

mia at the doses required for the treatment of hyperproliferative diseases such as cancer.[3] This limitation has led to intense synthetic efforts towards VDR ligands with selective activities as potential therapeutic agents for the treatment of cancer, immunodeficiency syndromes, autoimmune diseases and skin disorders.[5] Calcipotriol and maxacalcitol, examples of 1,25D analogs with a modified side-chain, exhibit similar or higher antiproliferative potency with reduced calcemic effects in comparison with natural hormone 1,25D (Figure 1).[6] Other potent 1,25D analogs structurally modified at the CD-rings or triene system that induce low potency for calcium metabolism have also been synthesized. Representative examples of these compounds include inecalcitol (19-nor-14-epi-23-yne-1,25D, TX522)[7] and PG-136,[8] which exhibit anticancer properties, and paricalcitol (19-nor-1,25D), which induces immunomodulatory effects and was recently proposed as a therapeutic option for patients with severe COVID-19.[9] Unfortunately, the mechanism underlying the dissociation of the antiproliferative effects from the calcemic effects, as well as the conformational requirements for selective biological functions, have not yet been established.[10]

The crystallographic structures of 1,25D and various of its analogs in complex with the VDR ligand binding domain indicate that the corresponding side-chain-C25OH groups adopt similar positions.[11] However, the side-chain flexibility makes difficult to predict the conformation associated with a particular biological function. Okamura and coworkers, in efforts to understand structure-activity relationships, pioneered the synthesis of 1,25D analogs with rigid structural units at the side chain to restrict its conformational mobility.[12] In the search for vitamin D analogs with an even higher degree of restricted mobility of the side chain, we have started a research program on the synthesis and biological evaluation of 1,25D analogs with locked units at the side chains attached to the D-ring, in the form of double bond,[13] cyclopropane ring,[14] aromatic ring,[15] and triple bond.[16] In connection with this program, we describe here the development of the first side-chain analogs of 1,25D that incorporate an allenic unit at C17 as the structural element to impart restricted mobility to the side chain.

Results and Discussion

Design

Based on the crystal structure of the active *h*VDR ligand-binding domain (LBD) bound to 1,25D,[11a] we studied the docking of the analogs **2a**–**2e** bearing an allenic unit at the side chain attached to C17 of the D-ring (Figure 1). We showed that analog **2d** binds well (97%) to the VDR LBD in comparison with the native hormone 1,25D (100%) (Figure 2). This analog adopts the canonical active conformation as the natural hormone in the binding pocked, where the A, C and D rings, and the triene system occupy similar positions. The A-ring and side-chain hydroxyl groups form effective hydrogen bonds with the same amino acid residues (His-305, His-397, Ser-278, Arg-274, Tyr-143, Ser-237) as the natural hormone. The other allenic analogs **2a** (87%), **2b** (92%), **2c** (86%), and **2e** (84%) bind to the *h*VDR LBD less efficiently than **2d**. On the basis of the in silico binding results, we chose compounds **2a**, **2b** and **2d** as the synthetic targets.

Retrosynthetic analysis of target compounds

The synthetic plan for the synthesis of target compounds **2a**, **2b**, and **2d** is outlined in Scheme 1. The formation of the vitamin D triene system involves a stereoselective Pd^0-catalyzed ring closure of enoltriflate **4** and subsequent Suzuki-Miyaura coupling with unprotected alkenyl-boronic ester **3** in protic medium following procedures developed in this laboratory.[17] At this point, the stability of the allenic unit under the Pd-catalyzed reaction conditions was uncertain. The boronates **3** are envisaged to arise from the allene **5** by conventional

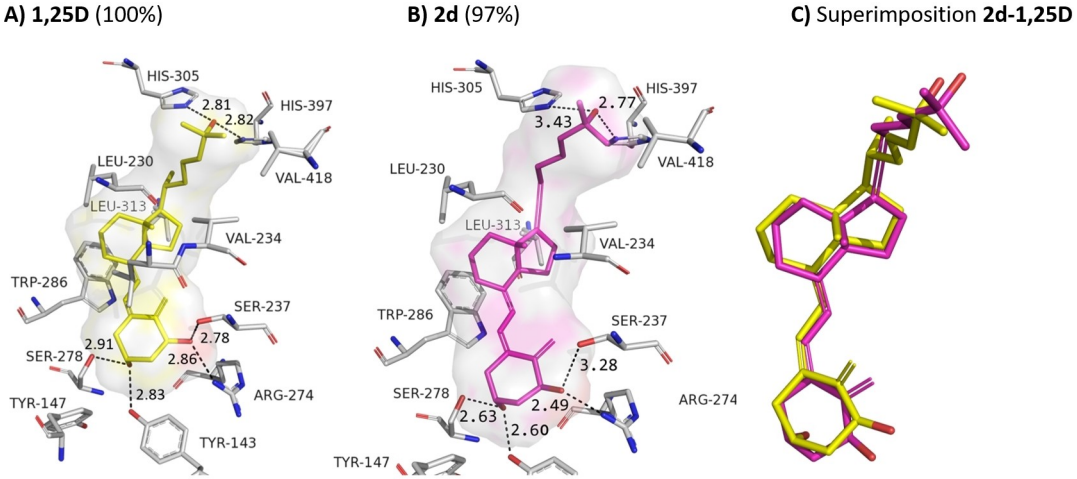

Figure 2. A) Structure of the natural hormone 1,25D (yellow) in complex with hVDR LBD (PDB ID: 1DB1). B) Docked structure of analog **2d** (magenta) into the hVDR LBD. **C)** Superimposition of both 1,25D and **2d**. Ligand-amino acid distances are shown in Å.

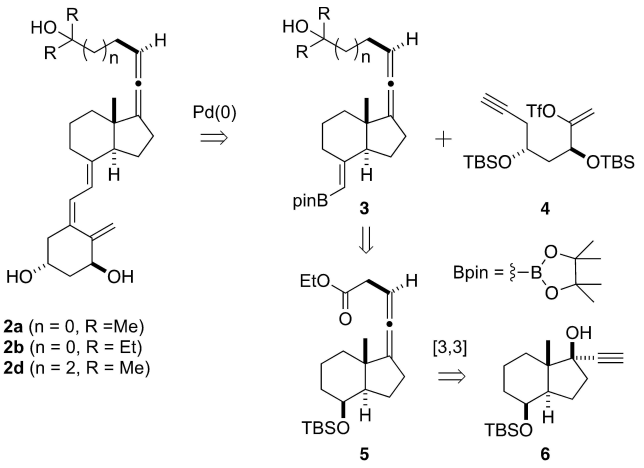

Scheme 1. Retrosynthesis of target analogs **2a**, **2b**, and **2d** from enoltriflate **4** and propargylic alcohol **6**.

chemistry. The key allene **5** would arise from propargylic alcohol **6** through an orthoester-Claisen rearrangement.[18] Compound **6** would be prepared in several steps by degradation of vitamin D_2.[19]

Synthesis of the upper boronate fragments

The synthesis of boronates **3a**, **3b**, and **3d** is outlined in Scheme 2. Reaction of ketone **7** with lithium trimethylsilylacetylide in THF followed by desilylation with Na_2CO_3 in methanol provided propargylic alcohol **6**[20] in 86% yield. Exposure of **6** to orthoester Claisen rearrangement with triethyl orthoacetate and acetic acid delivered the (*S*)-allene **5** (84%) as a single isomer [^{1}H NMR δ 5.27 (C=C=CH)]. Treatment of **5** with methyl magnesium bromide in THF provided the tertiary alcohol **8a** (98%), which was deprotected to alcohol **9a** (98%) with tetrabutylammonium fluoride in THF. Pyridinium dichromate oxidation of **9a** in CH_2Cl_2 followed by Wittig-olefination of the resulting ketone **10a** with ylide Ph_3P=CHBr,[21] prepared from $(Ph_3PCH_2Br)Br$ and KO*t*Bu in toluene, led to (*E*)-alkenyl bromide **11a** in 69% yield (two steps), which was converted to the desired upper boronate **3a** (58% yield) without protection of the side-chain-hydroxyl group by Miyaura's modified method[17,22] using bis(pinacolato)diboron and KOAc in the presence of catalytic [1,1'bis(diphenylphosphino) ferrocene] dichloropalladium(II) in DMSO.

The synthesis of boronate **3d** began with ester **5**, which was converted to iodide **13** by a three steps sequence (81% yield) involving reduction with diisobutylaluminum hydride in THF, treatment of the resulting alcohol **12** with *p*-toluenesulfonyl chloride in pyridine, and subsequent reaction of the resulting

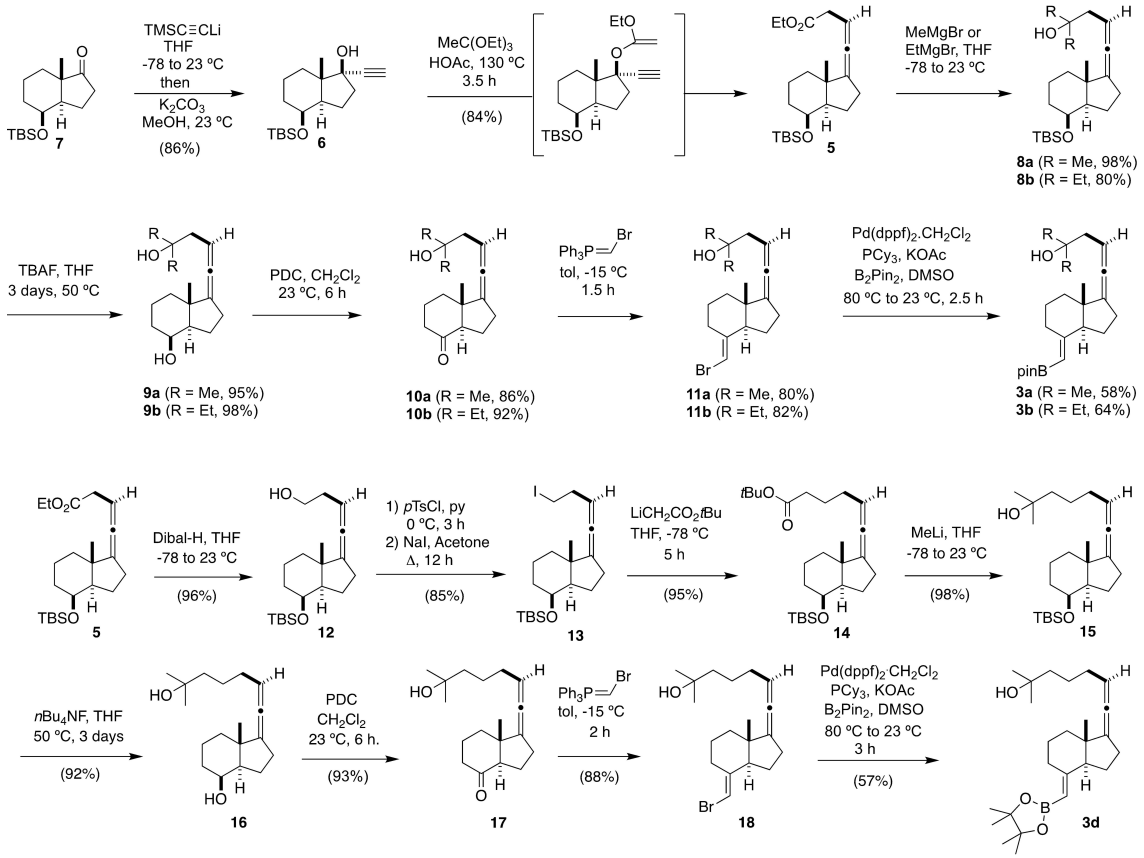

Scheme 2. Synthesis of the upper boronates **3a**, **3b**, and **3d**.

tosylate with sodium iodide in acetone. Chain extension by reaction of iodide **13** with the lithium anion derived from *tert*-butyl acetate in THF provided ester **14** in 95% yield, which was converted to diol **16** (90%) by methylation (MeLi, THF) and subsequent deprotection (nBu$_4$NF, THF). Pyridinium dichromate oxidation of **16** in CH_2Cl_2 and subsequent Wittig-olefination of the resulting ketone **17** with ylide Ph_3P=CHBr afforded the (*E*)-alkenyl bromide **18** in 82% yield (two steps), which was transformed into the desired upper boronate **3d** (57% yield) by reaction with bis(pinacolato)diboron and KOAc in the presence of catalytic [1,1'bis(diphenylphosphino) ferrocene] dichloropalladium(II) in DMSO as above (23.3% overall yield from ketone **7**, 12 steps). The allene moiety survived the Pd-catalyzed process during the formation of the vitamin D triene system though in moderate yield.[23]

Synthesis of target compounds

With the upper fragments in hand, we proceeded to the final convergent formation of the triene system of the target compounds **2a**, **2b**, and **2d** (Scheme 3). Pd-catalyzed carbocyclization of enoltriflate **4** (1.1 equiv) and subsequent Suzuki-Miyaura coupling with boronate **3a** (1 equiv) in the presence of catalytic bis(triphenylphosphine)palladium(II) in aqueous K_3PO_4 (2 M)/THF provided, after deprotection, the desired 1,25D-analog **2a** in 51% yield (two steps) (13.7% overall yield from ketone **7**, 14 steps). Same procedure was used for the preparation of allenic analog **2b** (16.4% overall yield from ketone **7**, 14 steps). In a similar way, Pd-catalyzed carbocyclization/Suzuki-Miyaura cross coupling tandem process on **3c** provided the protected 1,25D-analog **19**, which upon desilylation, gave the desired allenic 1,25D-analog **2d** (54%, two steps) (14.5% overall yield from ketone **7**, 14 steps).

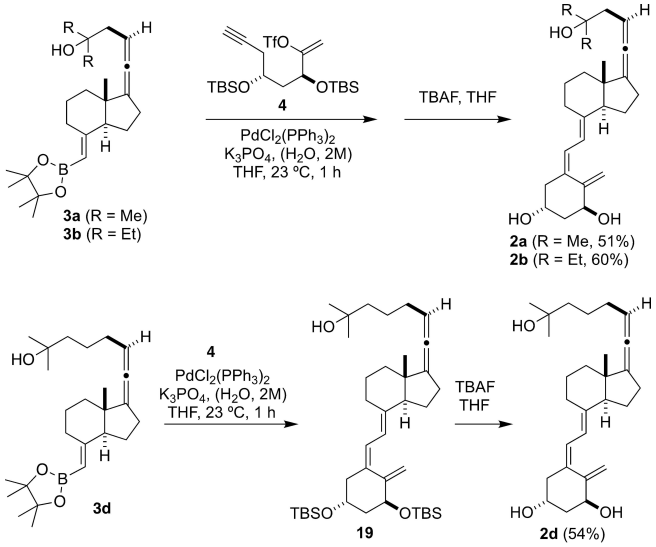

Scheme 3. Synthesis of the target vitamin D analogs **2a**, **2b**, and **2d**.

Functional activity

As the in silico data indicate that the allene **2d** binds to VDR with the highest efficiency, we determined its biological properties. Transactivation assay in HeLa cells transfected with human full length VDR showed that 1,25D (**1**) and **2d** induce the expression of a luciferase reporter gene under the control of the promoter of human *CYP24A1*, the main vitamin D target gene (Figure 3, A). Note that at lower doses, **2d** was less potent than **1**. In addition, we monitor the expression of *CYP24A1* transcripts in cells derived from prostate cancer metastasis (DU-145) treated for 24 h. Ligands **2d** and **1** induced transcript levels at 100 nM and 10 nM, but the levels were lower in cells treated with **2** (Figure 3, B).

To determine the effects of **2d** in vivo, wild type mice were daily treated with various doses of **2d** and **1** for 5 days. In agreement with previous results,[24] 1 μg/kg of **1** induced hypercalcemia and the transcript levels of the vitamin D target genes *Cyp24a1* and *S100g* in the kidney (Figure 3, D–E). However, the renal transcript levels were similar in mice treated with **2d** and with vehicle (Figure 3, D–E). The calcemic activity of **2d** was evaluated by monitoring the serum calcium levels in the treated mice (Figure 3, C). Serum calcium levels were unaffected at 1 and 3 μg/kg. Thus, these results indicate that **2d** is less potent than 1,25D, but behaves as a low-calcemic 1,25D analog.

Crystal structure

To determine the binding pose of the analog **2d**, we co-crystallized the zebrafish wild-type VDR LBD[11c] in complex with

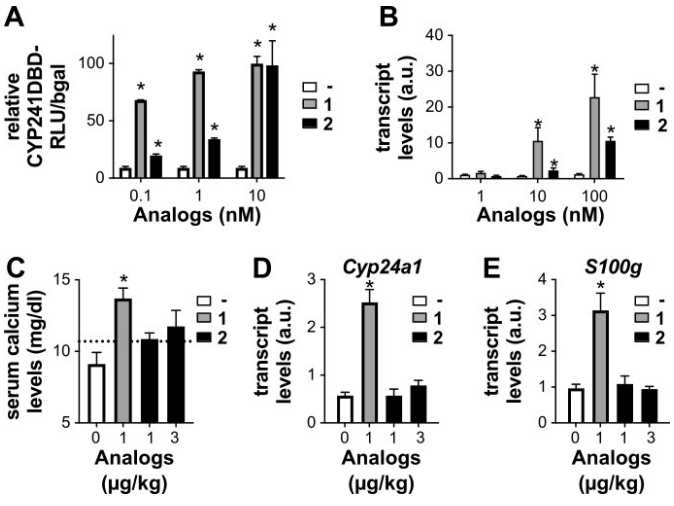

Figure 3. A) Transactivation assay in HeLa cells, transfected with full-length human VDR and a luciferase reporter gene under the control of the human *CYP24A1* promoter, and treated for 24 h with 1,25D (**1**) or **2d** at various concentrations. B) *CYP24A1* transcript levels in DU-145 cells treated for 24 h with **1** or **2d** at various concentrations. EtOH was used as solvent (−). Serum calcium levels (C) and renal transcript levels of *Cyp24a1* (D) and *S100g* (E) determined in wild type mice, 6 h after 5 daily administrations of **2d** or **1** at the indicated doses. Oil was used as vehicle (0 or -). * $p < 0.05$ vs. vehicle.

the ligand and a coactivator peptide and solved the structure with a resolution up to 2.1 Å (Supporting Table 1). The overall structure is highly homologous to the VDR-1,25D structure with a root mean square deviation of 0.3 Å over 235 residues when comparing the Cα atoms of the two complexes. Superposition of the VDR ligand binding pocket in the presence of **2d** and 1,25D shows similar positioning of the ligands (Figure 4, A), in agreement with the in silico docking data. The C1-OH, C3-OH and C25-OH groups of **2d** form similar H-bonds as 1,25D (Figure 4A), however the C25-OH forms weaker H-bonds with His-333 and His-423 (3.2 Å and 3.0 Å for analog **2d** compared to 2.8 Å and 2.8 Å for 1,25D). The secosteroidal part of the ligand forms similar interactions with the zVDR ligand binding pocket compared to 1,25D. The side chain of **2** forms extensive interactions with Leu-255, Leu-258, Val-262, Ala-331, His-333, His-423, Tyr-427, Leu-430 at a 4.0 Å distance cutoff (Figure 4, B). The difference in side chain position as a consequence of the rigid allenic unit attached to C17, results in a loss of interaction to residue Leu-337 in complex with **2d**. Overall, the contacts formed by **2d** in the zVDR complex stabilize the agonist conformation of VDR in agreement with the agonist potency of this novel compound. The weaker hydrogen bonds with His-333 and His-423 and loss of interaction with Leu-337 explain the observed difference in activity between the 1,25D and compound **2d**.

Conclusion

In summary, we have designed and synthesized three analogs of the hormone 1α,25-dihydroxyvitamin D_3 bearing an allenic unit attached to C17 as the structural element to impart conformational rigidity near the D-ring. Highlights of the synthetic route (about 14% overall yield from bicyclic ketone **7**, 14 steps), include the access to the allenic moiety by an orthoester-Claisen rearrangement and the formation of the triene system by a Pd^0-catalyzed cyclization/cross coupling process involving an enoltriflate, precursor of the A-ring, and a vinyl boronate containing an allenic side-chain unit corresponding to the CD-Side chain framework. Biological evaluation of **2d** with the highest affinity for VDR, reveals that the geometry imposed by the C17-allene moiety reduces the transcriptional potency and calcemic activity. The crystallographic structure of **2d** in complex with the VDR LBD provides information concerning side-chain conformational requirements for the design of new noncalcemic vitamin D analogs of potential therapeutic interest.

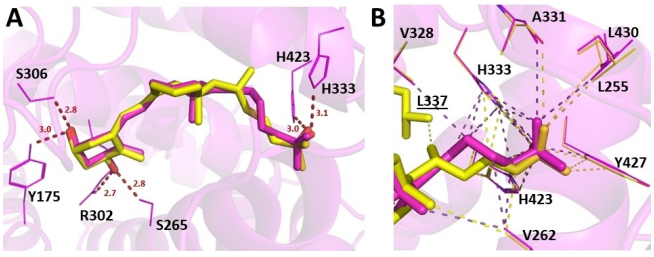

Figure 4. A) Overlay of 1,25D (carbon atoms in yellow and oxygen atoms in red) with analog **2d** (carbon atoms in magenta and oxygen atoms in red) within zVDR LBD complexes. Hydrogen bonds are depicted by red dashed lines and labeled with distances in Å. B) Details of the interactions mediated by the side chain of ligand **2d** and of 1,25D with residues of the zVDR LBD at a 4 Å distance cutoff, and shown by yellow and magenta dashed lines, respectively.

Experimental Section

General: For details on the general materials and methods, see Supporting Information.

Acknowledgements

We thank FCT of Portugal (project PTDC/BIA-MIB/29059/2017), UIDB/50006/2020 to LAQV-REQUIMTE Research Unit, the European Union (European Regional Development Fund-ERDF), and Xunta de Galicia, Spain (GRC/ED431B/2018/13), for financial support. We also thank the Ligue contre le cancer, Agence Nationale de la Recherche ANR-13-BSV8-0024-01, and institucional funds from Instruct-ERIC for support and use of resources of the French Infrastructure for Integrated Structural Biology (ANR-10-LABX-0030-INRT and ANR-10-IDEX-0002-02). ERB and JL thank FCT (SFRH/BSAB/150309/2019) and (PTDC/BIA-MIB/29059, 2017-REQUIMTE2019-86) for postdoctoral fellowships, respectively. We thank Dishman-Netherlands B.V. for the gift of vitamin D_2, P. Eberling for peptide synthesis, A. McEwen for help in X-ray data collection, C. Peluso-Iltis for excellent technical assistance, and the staff of PX2 beamline of SOLEIL synchrotron for assistance during X-ray data collection.

Conflict of Interest

The authors declare no conflict of interest.

Keywords: allenes · orthoester-Claisen rearrangement · Pd-catalyzed reactions · synthesis · vitamin D analogs

[1] R. M. Evans, *Science* **1988**, *240*, 889–895.
[2] M. R. Haussler, G. K. Whitfield, I. Kaneko, C. A. Haussler, D. Hsieh, J. C. Hsieh, P. W. Jurutka, *Calcif. Tissue Int.* **2013**, *92*, 77–98.
[3] a) R. Bouillon, W. H. Okamura, A. W. Norman, *Endocr. Rev.* **1995**, *16*, 200–257; b) Vitamin D (Eds.: D. Feldman, F. H. Glorieux, J. W. Pike), Academic Press, New York, **1997**; c) Vitamin D (Eds.: D. Feldman, J. W. Pike, J. S. Adams). Two-Volume Set, Elsevier, Academic Press, New York, **2011**.
[4] S. V. Ramagopalan, A. Heger, A. J. Berlanga, N. J. Maugeri, M. R. Lincoln, A. Burrell, L. Handunnetthi, A. E. Handel, G. Disanto, S–M. Orton, C. T. Watson, J. M. Morahan, G. Giovannoni, C. P. Ponting, G. C. Ebers, *Genome Res.* **2010**, *20*, 1352–1360.
[5] a) L. L. Issa, G. M. Leong, R. L. Sutherland, J. A. Eisman, *J. Bone Miner. Res.* **2002**, *17*, 879–890; b) A. Lori, L. A. Plum, H. F. DeLuca, *Nat. Drug Discov.* **2010**, *9*, 941–955; c) C. Leyssens, L. Verlinden, M. Verstuyf, *Front. Plant Physiol.* **2014**, *5*, 1–18.
[6] a) J. L. O'Neill, S. R. Feldman, *Drugs Today* **2010**, *46*, 351–60; b) M. A. Maestro, F. Molnár, C. Carlberg, *J. Med. Chem.* **2019**, *62*, 6854–6875.

[7] L. Verlinden, A. Verstuyf, M. Van Camp, S. Marcelis, K. Sabbe, X.-Y. Zhao, P. De Clercq, M. Vandewalle, R. Bouillon, *Cancer Res.* **2000**, *60*, 2673–2679.
[8] P. Gogoi, S. Seoane, R. Sigüeiro, T. Guiberteau, M. A. Maestro, R. Pérez-Fernández, N. Rochel, A. Mouriño, *J. Med. Chem.* **2018**. *61*, 4928–4937.
[9] R. M. Evans, S. M. Lippman, *Cell Metab.* **2020**, *32*, 704–709.
[10] A. Y. Belorusova, N. Rochel, *Structural Basis for Ligand Activity in Vitamin D*, Vol. 1 (Eds: D. Feldman). Academic Press **2018**, pp. 189–209.
[11] a) N. Rochel, J. M. Wurtz, A. Mitschler, B. Klaholz, D. Moras, *Mol. Cell* **2000**, *5*, 173–179; b) G. Tocchini-Valentini, N. Rochel, J. M. Wurtz, A. Mitschler, D. Moras, *Proc. Nat. Acad. Sci.* **2001**, *98*, 5491–5496; c) F. Ciesielski, N. Rochel, D. Moras, *J. Steroid Biochem. Mol. Biol.* **2007**, *103*, 235–242; d) C. Carlberg, F. Molnár, A. Mouriño, *Expert Opin. Ther. Pat.* **2012**, *22*, 417–435.
[12] a) B. Figadère, A. W. Norman, H. L. Henry, H. P. Koeffler, J-Y. Zhou, W. H. Okamura, *J. Med. Chem.* **1991**, *34*, 2452–2463; b) A. S. Craig, A. W. Norman, W. H. Okamura, *J. Org. Chem.* **1992**, *57*, 4374–4380; c) E. D. Collins, J. E. Bishop, C. M. Bula, A. Acevedo, W. H. Okamura, A. W. Norman, *J. Steroid Biochem. Mol. Biol.* **2005**, *94*, 279–288.
[13] J. A. Martínez-Pérez, L. Sarandeses, J. Granja, J. A. Palenzuela, A. Mouriño, *Tetrahedron Lett.* **1998**, *39*, 4725–4728.
[14] R. Riveiros, A. Rumbo, A. Sarandeses, A. Mouriño, *J. Org. Chem.* **2007**, *72*, 5477–5485.
[15] A. Fernández-Gacio, C. Vitale, A. Mouriño, *J. Org. Chem.* **2000**, *65*, 6978–6983.
[16] a) X. Pérez-García, A. Rumbo, M. J. Larriba, P. Ordóñez, A. Muñoz, A. Mouriño, *Org. Lett.* **2003**, *5*, 4033–4036; b) N. Rochel, S. Hourai, X. Pérez-García, A. Rumbo, A. Mourino, D. Moras, *Arch. Biochem. Biophys.* **2007**, *460*, 172–176; c) R. Sigüeiro, M. A. Maestro, A. Mouriño, *Org. Lett.* **2018**, *20*, 2641–2644.
[17] a) P. Gogoi, R. Sigüeiro, S. Eduardo, A. Mouriño, *Chem. Eur. J.* **2010**, *16*, 1432–1435; b) D. Carballa, R. Sigüeiro, Z. Rodriguez-Docampo, F. Zacconi, M. A. Maestro, A. Mouriño, *Chem. Eur. J.* **2018**, *24*, 3314–3320.
[18] R. R. Fernandes, A. K. Chowdhury, P. Kattanguru, *Eur. J. Org. Chem.* **2014**, *2014*, 2833–2871.
[19] E. Moman, D. Nicoletti, A. Mouriño, *J. Org. Chem.* **2004**, *69*, 4615–4625.
[20] C. Fernández, O. Diouf, E. Momán, G. Gómez, Y. Fall, *Synthesis* **2005**, *10*, 1701–1705.
[21] B. M. Trost, J. Dumas, M. Villa, *J. Am. Chem. Soc.* **1992**, *114*, 9836–9845.
[22] T. Ishiyama, T. Murata, M. Miyaura, *J. Org. Chem.* **1995**, *60*, 7508–7510.
[23] For a review on the chemistry of allenes, see: J. Ye, S. Ma, *Acc. Chem. Res.* **2014**, *47*, 989–1000.
[24] D. Rovito, A. Y. Belorusova, S. Chalhoub, A. I. Rerra, E. Guiot, A. Molin, A. Linglart, N. Rochel, G. Laverny, D. Metzger, *Nat. Commun.* **2020** *11*, 6249–6260.

Manuscript received: May 4, 2021
Accepted manuscript online: July 5, 2021
Version of record online: August 11, 2021

